Diabetologia (2024) 67:2786–2803
https://doi.org/10.1007/s00125-024-06232-2

ARTICLE

Deletion of *RFX6* impairs iPSC-derived islet organoid development and survival, with no impact on PDX1$^+$/NKX6.1$^+$ progenitors

Noura Aldous[1,2,3] · Ahmed K. Elsayed[1,2,4] · Bushra Memon[3] · Sadaf Ijaz[5] · Sikander Hayat[5] · Essam M. Abdelalim[1,2,3]

Received: 6 March 2024 / Accepted: 11 June 2024 / Published online: 30 July 2024

Abstract

Aims/hypothesis Homozygous mutations in *RFX6* lead to neonatal diabetes accompanied by a hypoplastic pancreas, whereas heterozygous mutations cause MODY. Recent studies have also shown *RFX6* variants to be linked with type 2 diabetes. Despite *RFX6*'s known function in islet development, its specific role in diabetes pathogenesis remains unclear. Here, we aimed to understand the mechanisms underlying the impairment of pancreatic islet development and subsequent hypoplasia due to loss-of-function mutations in *RFX6*.

Methods We examined regulatory factor X6 (RFX6) expression during human embryonic stem cell (hESC) differentiation into pancreatic islets and re-analysed a single-cell RNA-seq dataset to identify RFX6-specific cell populations during islet development. Furthermore, induced pluripotent stem cell (iPSC) lines lacking RFX6 were generated using CRISPR/Cas9. Various approaches were then employed to explore the consequences of RFX6 loss across different developmental stages. Subsequently, we evaluated transcriptional changes resulting from RFX6 loss through RNA-seq of pancreatic progenitors (PPs) and endocrine progenitors (EPs).

Results RFX6 expression was detected in PDX1$^+$ cells in the hESC-derived posterior foregut (PF). However, in the PPs, RFX6 did not co-localise with pancreatic and duodenal homeobox 1 (PDX1) or NK homeobox 1 (NKX6.1) but instead co-localised with neurogenin 3, NK2 homeobox 2 and islet hormones in the EPs and islets. Single-cell analysis revealed high *RFX6* expression levels in endocrine clusters across various hESC-derived pancreatic differentiation stages. Upon differentiating iPSCs lacking RFX6 into pancreatic islets, a significant decrease in PDX1 expression at the PF stage was observed, although this did not affect PPs co-expressing PDX1 and NKX6.1. RNA-seq analysis showed the downregulation of essential genes involved in pancreatic endocrine differentiation, insulin secretion and ion transport due to RFX6 deficiency. Furthermore, RFX6 deficiency resulted in the formation of smaller islet organoids due to increased cellular apoptosis, linked to reduced catalase expression, implying a protective role for RFX6. Overexpression of RFX6 reversed defective phenotypes in *RFX6*-knockout PPs, EPs and islets.

Conclusions/interpretation These findings suggest that pancreatic hypoplasia and reduced islet cell formation associated with RFX6 mutations are not due to alterations in PDX1$^+$/NKX6.1$^+$ PPs but instead result from cellular apoptosis and downregulation of pancreatic endocrine genes.

Data availability RNA-seq datasets have been deposited in the Zenodo repository with accession link (DOI: https://doi.org/10.5281/zenodo.10656891).

Keywords Diabetes · Endocrine specification · Islet organoids · Pancreatic hypoplasia · Pancreatic progenitors · Transcription factors

✉ Essam M. Abdelalim
emohamed3@sidra.org

[1] College of Health and Life Sciences, Hamad Bin Khalifa University (HBKU), Qatar Foundation (QF), Education City, Doha, Qatar

[2] Laboratory of Pluripotent Stem Cell Disease Modeling, Translational Medicine Department, Research Branch, Sidra Medicine, Doha, Qatar

[3] Diabetes Research Center, Qatar Biomedical Research Institute (QBRI), Hamad Bin Khalifa University (HBKU), Qatar Foundation (QF), Doha, Qatar

[4] Stem Cell Core, Qatar Biomedical Research Institute (QBRI), Hamad Bin Khalifa University (HBKU), Qatar Foundation (QF), Doha, Qatar

[5] Department of Medicine 2 (Nephrology, Rheumatology, Clinical Immunology and Hypertension), RWTH Aachen University, Medical Faculty, Aachen, Germany

Research in context

What is already known about this subject?

- Biallelic mutation in *RFX6* leads to permanent neonatal diabetes associated with hypoplastic pancreas
- *RFX6* expression starts during the posterior foregut stage and plays an important role in the development of human pancreatic islet cells
- *RFX6* knockout during human pancreatic islet differentiation results in reduction of PDX1 and absence of pancreatic beta cells

What is the key question?

- What mechanisms underlie the impairment of pancreatic islet development and subsequent hypoplasia due to loss-of-function mutations in *RFX6*?

What are the new findings?

- The absence of RFX6 did not impair induced pluripotent stem cell differentiation into pancreatic progenitors co-expressing PDX1 and NK6 homeobox 1
- During pancreatic differentiation, a lack of RFX6 resulted in the formation of hypoplastic islet organoids, potentially triggered by increased cellular apoptosis
- Cell death associated with the absence of RFX6 was mainly due to deficiency of the antioxidant enzyme catalase

How might this impact on clinical practice in the foreseeable future?

- Increasing the levels of the antioxidant enzyme catalase in pancreatic cells lacking RFX6 may serve as a potential therapeutic target for diabetes patients with RFX6 defects

Abbreviations

CAT	Catalase
CDX2	Caudal type homeobox 2
CHGA	Chromogranin A
DEG	Differentially expressed gene
EEC	Enteroendocrine cell
EP	Endocrine progenitor
FOXA2	Forkhead box A2
GCG	Glucagon
GIP	Gastric inhibitory polypeptide
GO	Gene ontology
HA	Haemagglutinin
hESC	Human embryonic stem cell
INS	Insulin
iPSC	Induced pluripotent stem cell
KO	Knockout
MRS	Mitchell–Riley syndrome
NEUROG3	Neurogenin 3
NKX2.2	NK2 homeobox 2
NKX6.1	NK homeobox 1
PAX4	Paired box 4
PDX1	Pancreatic and duodenal homeobox 1
PF	Posterior foregut
PNDM	Permanent neonatal diabetes
PP	Pancreatic progenitor
PPY	Pancreatic polypeptide Y
RFX6	Regulatory factor X6
RFX6 OE	RFX6 overexpression
scRNA-seq	Single-cell RNA-seq
SOX	SRY-box transcription factor
SST	Somatostatin
UCN3	Urocortin 3
WT	Wild-type

Introduction

Regulatory factor X6 (RFX6), a critical transcription factor, is crucial for islet cell development and function. Homozygous mutations in *RFX6* cause Mitchell–Riley syndrome (MRS), which is characterised by severe neonatal diabetes associated with hypoplastic pancreas, and intestinal atresia [1–5]. It has been suggested that this form of diabetes is attributed to the overall impairment of pancreatic islet development and function, including a reduction in insulin (INS) production by beta cells [1, 6]. In contrast, heterozygous

mutations result in mild MODY [7–9], where defective INS secretion occurs despite normal islet development [4, 10]. Thus, it appears that RFX6 governs both islet development and INS production, albeit through different mechanisms. Knocking down RFX6 in human EndoC-βH1 cells alters *INS* mRNA levels [4]. Furthermore, genome-wide association studies link *RFX6* variants to type 2 diabetes [11] and analysis of multiomics data from individuals with type 2 diabetes reveals genetic regions enriched with RFX-binding motifs [12].

Mouse studies reveal that *Rfx6* expression initiates in gut endoderm, undergoes a developmental transition and becomes restricted to the endocrine lineage within the pancreas, persisting in adult islet cells. The significance of *Rfx6* in islet cell development is evident across various species [1, 2, 6, 13, 14]. In mice with *Rfx6* gene deficiency, all endocrine cells are absent, except for polypeptide-secreting cells, resulting in diabetes and early postnatal death, limiting the exploration of its role in beta cell function and INS production [1, 6]. In adult beta cells, the loss of *Rfx6* results in glucose intolerance, impaired glucose sensing and defective INS secretion [10]. Moreover, RFX6 is expressed in gastric inhibitory polypeptide (GIP)-positive enteroendocrine K cells, regulating GIP promoter activity [15]. Furthermore, a recent study demonstrated that the loss of *Rfx6* function in ex vivo mouse intestinal organoids reduces enteroendocrine cells (EECs) [16].

Mutations in *RFX6* have led to different types of diabetes [1], raising questions about its importance in pancreatic islet development and function. Understanding its role could lead to new diabetes treatments. While previous research shows RFX6 is crucial for islet development and glucose regulation, its exact involvement in diabetes is unclear. This study used CRISPR/Cas9 to generate induced pluripotent stem cells (iPSCs) lacking RFX6, then differentiating them into islet cells. We aimed to investigate the impact of RFX6 loss at different developmental stages to determine the role of RFX6 in endocrine pancreatic development and islet survival.

Methods

Culture of human embryonic stem cells and induced pluripotent stem cells HA-RFX6 tagged H9 human embryonic stem cell (hESC) line (*RFX6*$^{HA/HA}$ H9-hESCs) and its control, H9-hESCs, were obtained from N. R. Dunn (A*STAR, Singapore). Wild-type (WT) induced pluripotent stem cells (iPSCs) generated in our laboratory were used [17, 18]. All cells were cultured in mTeSR Plus medium (Stem Cell Technologies, Canada) on Matrigel-coated dishes (Corning, USA) [19, 20].

Differentiation of hESCs and iPSCs into pancreatic islets hESC/iPSC lines were differentiated in vitro into pancreatic progenitors (PPs) using our protocol [21]. The protocol of Veres et al was adapted for further differentiation into pancreatic islet cells [22]. See electronic supplementary material (ESM) Methods and ESM Table 1 for details.

Generation of *RFX6*-knockout iPSCs We generated two *RFX6*-knockout (KO) human iPSC lines (RFX6 KO1 and RFX6 KO2) from WT iPSCs using Lipofectamine 3000 Transfection Reagent (ThermoFisher Scientific, Waltham, MA, USA) for the GFP-tagged plasmid vector expressing spCas9 and gRNA. Cells were sorted based on GFP expression at 48 h post-transfection.

Paraffin embedding and immunofluorescence We performed immunostaining as reported previously [19] and used the paraffin embedding technique for 3D pancreatic islet organoids following established protocols [23, 24]. See ESM Methods and ESM Table 2 for details.

Flow cytometry, western blotting, PCR and RT-PCR Flow cytometry, western blotting, PCR and RT-PCR were conducted as reported previously. See ESM Methods and ESM Tables 2, 3 for details.

Single-cell and RNA-seq analyses We used the GSE202497 dataset for single-cell analysis (https://www.ncbi.nlm.nih.gov/geo/query/acc.cgi?acc=GSE202497) [25]. Further details on single-cell and RNA-seq analyses are available in ESM Methods.

Apoptosis and proliferation assays The apoptosis and proliferation assays were performed, following previously established protocols [26] (see ESM Methods).

***RFX6* overexpression** RFX6 overexpression was induced as previously reported [26] (see ESM Methods).

Analysis of protein–protein interaction networks associated with *CAT* To explore *CAT* interactions and predict functional associations, we employed the STRING database (https://string-db.org) [27].

Statistical analysis At least three biological replicates were used in most experiments while statistical analysis was done using unpaired two-tailed Student's *t* test on Prism version

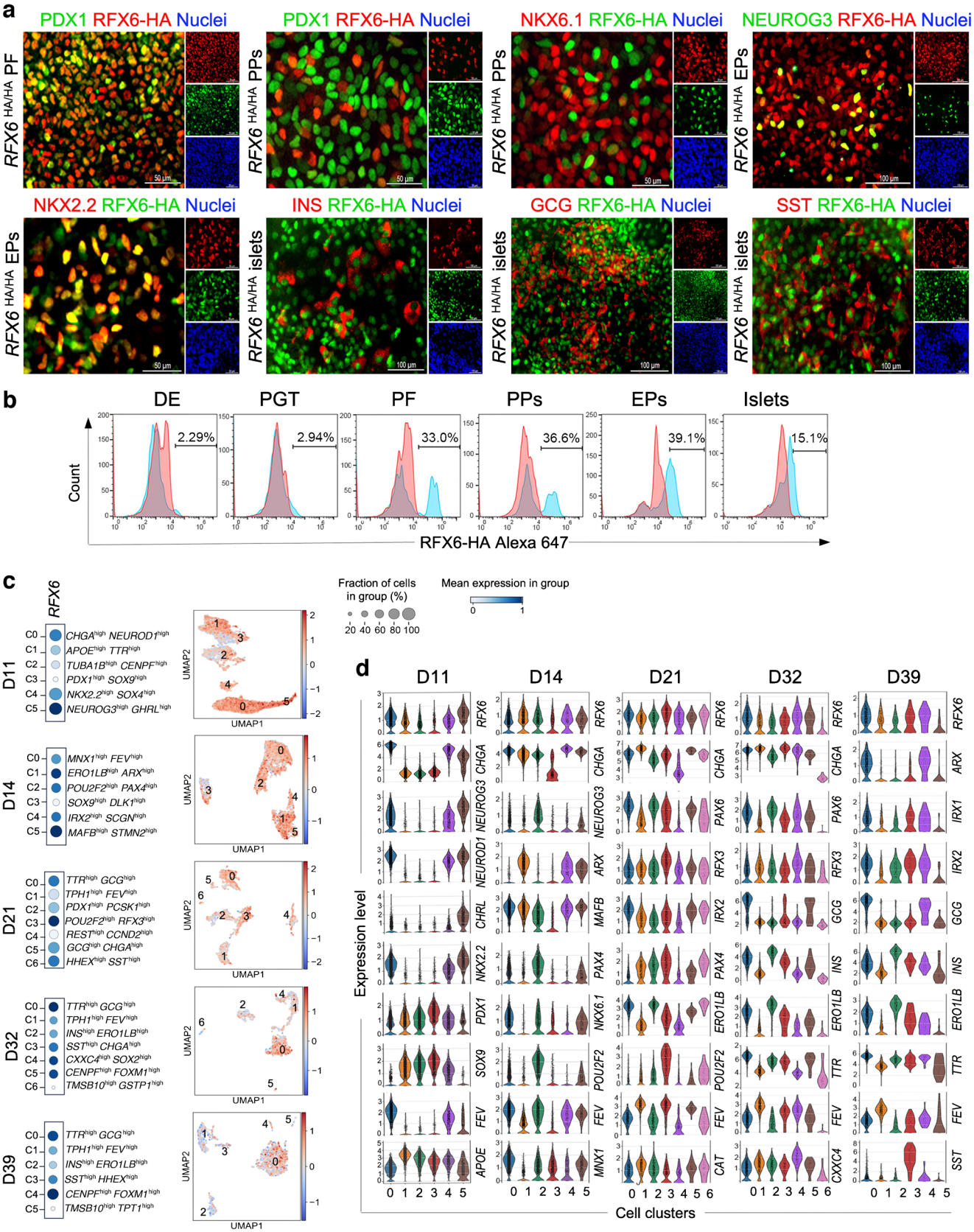
a
PDX1 RFX6-HA Nuclei
PDX1 RFX6-HA Nuclei
NKX6.1 RFX6-HA Nuclei
NEUROG3 RFX6-HA Nuclei
NKX2.2 RFX6-HA Nuclei
INS RFX6-HA Nuclei
GCG RFX6-HA Nuclei
SST RFX6-HA Nuclei
RFX6 HA/HA PF
RFX6 HA/HA PPs
RFX6 HA/HA PPs
RFX6 HA/HA EPs
RFX6 HA/HA EPs
RFX6 HA/HA islets
RFX6 HA/HA islets
RFX6 HA/HA islets
50 µm
100 µm
b
DE
PGT
PF
PPs
EPs
Islets
2.29%
2.94%
33.0%
36.6%
39.1%
15.1%
Count
RFX6-HA Alexa 647
c
RFX6
Fraction of cells in group (%)
20 40 60 80 100
Mean expression in group
0
1
D11
C0 CHGA^high NEUROD1^high
C1 APOE^high TTR^high
C2 TUBA1B^high CENPF^high
C3 PDX1^high SOX9^high
C4 NKX2.2^high SOX4^high
C5 NEUROG3^high GHRL^high
D14
C0 MNX1^high FEV^high
C1 ERO1LB^high ARX^high
C2 POU2F2^high PAX4^high
C3 SOX9^high DLK1^high
C4 IRX2^high SCGN^high
C5 MAFB^high STMN2^high
D21
C0 TTR^high GCG^high
C1 TPH1^high FEV^high
C2 PDX1^high PCSK1^high
C3 POU2F2^high RFX3^high
C4 REST^high CCND2^high
C5 GCG^high CHGA^high
C6 HHEX^high SST^high
D32
C0 TTR^high GCG^high
C1 TPH1^high FEV^high
C2 INS^high ERO1LB^high
C3 SST^high CHGA^high
C4 CXXC4^high SOX2^high
C5 CENPF^high FOXM1^high
C6 TMSB10^high GSTP1^high
D39
C0 TTR^high GCG^high
C1 TPH1^high FEV^high
C2 INS^high ERO1LB^high
C3 SST^high HHEX^high
C4 CENPF^high FOXM1^high
C5 TMSB10^high TPT1^high
UMAP1
UMAP2
d
D11
D14
D21
D32
D39
RFX6
CHGA
NEUROG3
NEUROD1
CHRL
NKX2.2
PDX1
SOX9
FEV
APOE
PAX6
RFX3
IRX2
PAX4
NKX6.1
POU2F2
MNX1
ARX
MAFB
CAT
GCG
INS
ERO1LB
TTR
CXXC4
SST
IRX1
Expression level
Cell clusters

◂**Fig. 1** Timeline expression and single-cell analysis of RFX6 throughout the differentiation of hESCs into various stages of pancreatic development. (**a**) Immunostaining showing the expression of RFX6 during differentiation of hESC-H9 into pancreatic islets. (**b**) Flow cytometric quantification of RFX6 expression during different stages of differentiation. (**c**) Dot plots and feature plots illustrating *RFX6* expression across distinct cell clusters. Each dot's colour and size correspond to the expression level and the percentage of cells expressing the *RFX6* gene. (**d**) The violin plots illustrate the expression distributions of key genes across various clusters at distinct stages of hESC differentiation into pancreatic islets: day 11 (D11); day 14 (D14); day 21 (D21); day 32 (D32); and day 39 (D39). DE, definitive endoderm; PGT, primitive gut tube. Scale bar, 100 μm

8 (GraphPad Software, Boston, MA, USA, www.graphpad.com), with data represented as mean ± SD.

Results

Temporal and cell-specific expression of RFX6 during pancreatic islet differentiation To examine RFX6 expression during pancreatic islet differentiation, we tracked its levels in hESC-H9 cells at various differentiation stages (ESM Fig. 1a). Due to the lack of a specific antibody for RFX6 immunostaining, we used a modified *RFX6*$^{HA/HA}$ hESC-H9 line, incorporating a triplicated haemagglutinin (HA) epitope to enable RFX6 protein detection [28]. Initially, RFX6 immunoreactivity was absent during the definitive endoderm and primitive gut tube stages (ESM Fig. 1b). However, robust expression emerged in the posterior foregut (PF), largely co-localised with pancreatic and duodenal homeobox 1 (PDX1) (Fig. 1a). Interestingly, while RFX6 persisted in the PP stage, it did not co-localise with PDX1 or NK6 homeobox 1 (NKX6.1) (Fig. 1a). During the endocrine progenitor (EP) stage, RFX6 co-localised with neurogenin 3 (NEUROG3) and NK2 homeobox 2 (NKX2.2), the pancreatic endocrine markers (Fig. 1a). In the islet cell stage, RFX6 co-expressed with INS, glucagon (GCG) and somatostatin (SST) (Fig. 1a). Flow cytometry analysis confirmed high RFX6 levels from the PF stage onwards, peaking at the EP stage (Fig. 1b). These findings suggest that RFX6 may not be indispensable for PDX1$^+$/NKX6.1$^+$ PPs.

To delve deeper into identifying specific cell populations expressing *RFX6*, we re-analysed the recently published single-cell (scRNA-seq) datasets of PPs at day 11 (D11), EPs at day 14 (D14), immature islets at day 21 (D21) and maturing islets at days 32 and 39 (D32 and D39), derived from hESCs [25]. We used unsupervised clustering to create 2D visualisations using uniform manifold approximation and projection (UMAP) plots and identified multiple cell populations at each differentiation stage (Fig. 1c, d and ESM Fig. 2). At D11, six cell clusters were identified, with three showing high expression levels of pancreatic endocrine markers. RFX6 was mainly expressed in these clusters, with the highest level in C5, distinguished by *NEUROG3*^{high}/GHRL^{high}, which also expressed high levels of other endocrine markers such as *PAX4*, *INSM1*, *KCNK17*, *NKX2.2* and *SOX4*. Moderate RFX6 expression was observed in two additional endocrine clusters (C0 and C4), characterised by *CHGA*^{high}/*NEUROD1*^{high} and *NKX2.2*^{high}/*SOX4*^{high}, respectively. Low *RFX6* expression was seen in C1 (*APOE*^{high}/*TTR*^{high}) and C2 (proliferation cluster; *TUBA1B*^{high}/*CENPF*^{high}). Almost no expression was detected in C3, identified by *PDX1*^{high}/*SOX9*^{high} (Fig. 1c, d and ESM Fig. 2). These findings strongly indicate that RFX6 expression in PPs is confined to endocrine cell populations.

At D14, we identified six clusters, with the highest expression of RFX6 observed in the endocrine cluster C5, marked by *MAFB*^{high}/*STMN2*^{high}; this cluster also showed elevated levels of essential endocrine markers such as *INS*, *GCG* and *SLC30A8* (Fig. 1c, d and ESM Fig. 2). Another endocrine cluster, C1 (*ERO1LB*^{high}/*ARX*^{high}), displayed high RFX6 expression levels. In addition, a moderate *RFX6* level was detected in C2 (*POU2F2*^{high}/*PAX4*^{high}), C0 (*MNX1*^{high}/*FEV*^{high}) and C4 (*IRX2*^{high}/*SCGN*^{high}). The lowest RFX6 expression was seen in C3 (PP cluster; *SOX9*^{high}/*DLK1*^{high}), which also expressed high levels of *PDX1*, *HNF1B*, *GATA4*, *TCF7L2* and *CCND2*. At D21, the highest expression of RFX6 was seen in C3 (*POU2F2*^{high}/*RFX3*^{high}), while a moderate expression was seen in C0 (*TTR*^{high}/*GCG*^{high}), C5 (*GCG*^{high}/*CHGA*^{high}) and C6 (delta cell cluster; *HHEX*^{high}/*SST*^{high}). Reduced expression was observed in C1 (*TPH1*^{high}/*FEV*^{high}), previously identified as a specific enterochromaffin progenitor population [29], and in C4 (proliferation cluster; *REST*^{high}/*CCND2*^{high}) (Fig. 1c, d and ESM Fig. 2).

At D32, the most significant RFX6 expression was seen in C0 (*TTR*^{high}/*GCG*^{high}) (Fig. 1c), which also expressed high levels of *CHGA*, *IRX2*, and *ARX*, suggesting an alpha cell fate. Moderate RFX6 expression was seen in C4 (*CXXC4*^{high}/*SOX2*^{high}) and C5 (proliferation cluster; *CENPF*^{high}/*FOXM1*^{high}), while lower levels were seen in C1 (*TPH1*^{high}/*FEV*^{high}) and C2 (*INS*^{high}/*ERO1LB*^{high}). *ERO1LB* (also known as *ERO1B*) is known as a gene specifically associated with pancreatic beta cells [30]. No expression was observed in C6 (*TMSB10*^{high}/*GSTP1*^{high}). At D39, the highest RFX6 expression was seen in C4 (proliferation cluster; *CENPF*^{high}/*FOXM1*^{high}), with moderate expression in C0 (*TTR*^{high}/*GCG*^{high}). Lower expression was seen

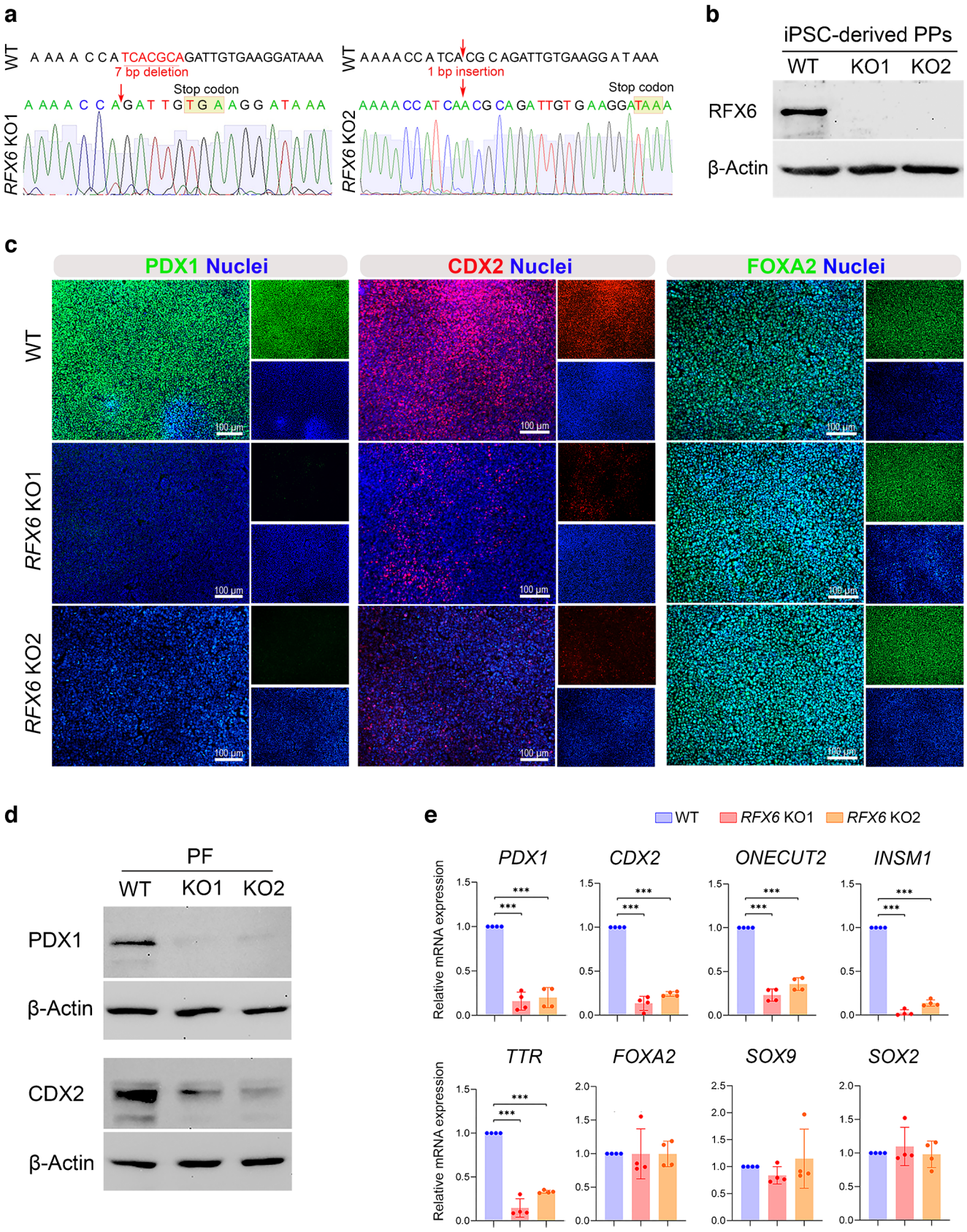
a
WT
A AA A C C A TCACGCAGATTGTGAAGGATAAA
7 bp deletion
Stop codon
A AA A C C A G A T T G T G A A G G A T A A A
RFX6 KO1
WT
A A A A CC A TCA CG C AGATTGTGAAGG A T AAA
1 bp insertion
Stop codon
A A A A CC AT CAA CG CA GA TTGT G A AGGATA A A
RFX6 KO2
b
iPSC-derived PPs
WT
KO1
KO2
RFX6
β-Actin
c
PDX1 Nuclei
CDX2 Nuclei
FOXA2 Nuclei
WT
RFX6 KO1
RFX6 KO2
100 μm
d
PF
WT
KO1
KO2
PDX1
β-Actin
CDX2
β-Actin
e
WT
RFX6 KO1
RFX6 KO2
PDX1
CDX2
ONECUT2
INSM1
TTR
FOXA2
SOX9
SOX2
Relative mRNA expression
***

◂**Fig. 2** Loss of *RFX6* reduces PDX1 and CDX2 expression in iPSC-derived PF. (**a**) DNA sequence confirmation of frameshift mutations in isogenic KO iPSC clones compared with WT iPSCs. (**b**) Western blot analysis confirming the absence of RFX6 protein in PPs derived from *RFX6* KO iPSC lines. (**c**) Immunofluorescence images showing the expression of PDX1, CDX2 and FOXA2 in PPs derived from WT iPSCs and *RFX6* KO iPSCs. (**d**) Western blot analysis showing the expression of PDX1 and CDX2 in *RFX6* KO PF compared with WT PF. (**e**) RT-qPCR analysis showing the mRNA expression of PF markers *PDX1*, *CDX2*, *ONECUT2*, *INSM1*, *TTR*, *FOXA2*, *SOX9* and *SOX2* in *RFX6* KO PF relative to WT control PF (n=4). The data are presented as mean ± SD. ***p<0.001. Scale bar, 100 μm

in C3 (SST^{high}/$HHEX^{high}$), C1 ($TPH1^{high}$/FEV^{high}) and C2 (INS^{high}/$ERO1LB^{high}$), while no expression was seen in C5 ($TMSB10^{high}$/$TPT1^{high}$) (Fig. 1c, d and ESM Fig. 2). Taken together, these findings indicate that RFX6 is mainly expressed in pancreatic endocrine cell populations across various stages and is not expressed in $PDX1^+$ cell populations within PPs.

Depletion of RFX6 diminishes PDX1 expression in the PF and does not affect PDX1$^+$/NKX6.1$^+$ PPs To explore RFX6's contribution to human pancreatic development and the generation of pancreatic islet cells, biallelic *RFX6* mutant human iPSC lines (referred to as *RFX6* KO iPSCs) were established using the CRISPR/Cas9 system. Mutations were introduced into the WT iPSC line generated in our laboratory [18] using a gRNA that targeted exon 2 of *RFX6*. The mutations were validated through Sanger sequencing and were anticipated to induce a frameshift resulting in the formation of premature stop codons preventing RFX6 protein translation (Fig. 2a). The absence of RFX6 protein expression was confirmed in PPs derived from *RFX6* KO cell lines compared with WT controls using western blot analysis (Fig. 2b). All iPSC lines expressed pluripotency markers *OCT4* (also known as *POU5F1*), *NANOG*, *SOX2*, *SSEA4*, *TRA-1-60*, *TRA-81*, *C-MYC* (also known as *MYC*), *KLF4*, *REX1* (also known as *ZFP42*), *DPPA4* and *TERT* (ESM Fig. 3a, b). Moreover, they have been verified to maintain normal karyotypes consistent with the parental line and are free from mycoplasma (ESM Fig. 3c, d).

Next, we examined the effect of *RFX6* loss on pancreatic differentiation. Immunostaining and western blotting showed reduced PDX1 and caudal type homeobox 2 (CDX2) protein levels in *RFX6*-deficient PF cells, while forkhead box A2 (FOXA2) remained unchanged (Fig. 2c, d). qPCR analysis revealed significant downregulation in the mRNA expression of *PDX1*, *CDX2*, *ONECUT2*, *INSM1* and *TTR* in *RFX6* KO PF compared with WT PF (Fig. 2e). In contrast, *FOXA2*, *SOX9* and *SOX2* expression remained unaffected (Fig. 2e). Despite the dramatic reduction in PDX1 expression during the PF stage, *RFX6*-deficient iPSCs were able to produce PPs and co-expressed PDX1 and NKX6.1 like controls (Fig. 3a–d and ESM Fig. 4). Other PP markers, including SRY-box transcription factor (SOX)9 and FOXA2, remained unchanged, as evidenced by western blotting and RT-qPCR (Fig. 3c, d). These results suggest that RFX6 does not play a significant role in the formation of PDX1$^+$/NKX6.1$^+$ cells during the PP stage.

At the EP stage, we found that there was a dramatic reduction of the pan endocrine marker, CHGA (Fig. 3e, f), with no significant change in NKX6.1 and NKX2.2 expression (Fig. 3e). RT-qPCR analysis showed significant reduction in the expression of *NEUROD1*, while the expression of *NEUROG3*, *NKX2.2*, and *PAX4* were significantly increased in EPs lacking *RFX6* compared with WT controls (Fig. 3g).

Deletion of *RFX6* leads to large-scale transcriptomic alterations associated with pancreatic endocrine specification in PPs and EPs For comprehensive understanding of the transcriptomic changes between *RFX6* KO and WT cells, RNA-seq was performed on PPs and EPs. Our transcriptome analysis on iPSC-derived PPs detected 392 differentially expressed genes (DEGs) significantly affected by *RFX6* deletion. Among these DEGs, 223 genes were significantly downregulated ($\log_2$ fold change < −1.0, p<0.05), while 169 genes were significantly upregulated ($\log_2$ fold change >1.0, p<0.05) in *RFX6* KO PPs compared with WT PPs (Fig. 4a and ESM Fig. 5a). At the EP stage, we identified 325 DEGs significantly impacted by the deletion of *RFX6*, with 215 of these genes being significantly downregulated ($\log_2$ fold change < −1.0, p<0.05) and 110 genes being significantly upregulated ($\log_2$ fold change >1.0, p<0.05) in *RFX6* KO EPs compared with WT EPs (Fig. 4a and ESM Fig. 5b). Interestingly, 160 of the downregulated DEGs, comprising 57.3%, were found in both PPs and EPs (Fig. 4b), with most of these genes known to be associated with pancreatic endocrine development. The Gene Ontology (GO) of the downregulated DEGs in PPs and EPs displayed enriched genes linked to pancreatic endocrine development, INS secretion regulation, regulation of ion transmembrane transport and negative regulation of cell apoptosis (Fig. 4c and ESM Fig. 5c, d), whereas the upregulated DEGs showed GO enrichment in genes linked to lipid metabolism and nervous system development (data not shown). At the PP stage, the RT-qPCR validation analysis confirmed a significant decrease in the expression of endocrine genes including *ARX*, *PAX6*, *CHGA*, *IRX1*, *IRX2*, *INS*, *GCG*, *SST*, *MAF1B*, *ERO1B (ERO1LB)*, *NEUROD1*, *PCSK1*, *CRYBA2*, *SCGN*,

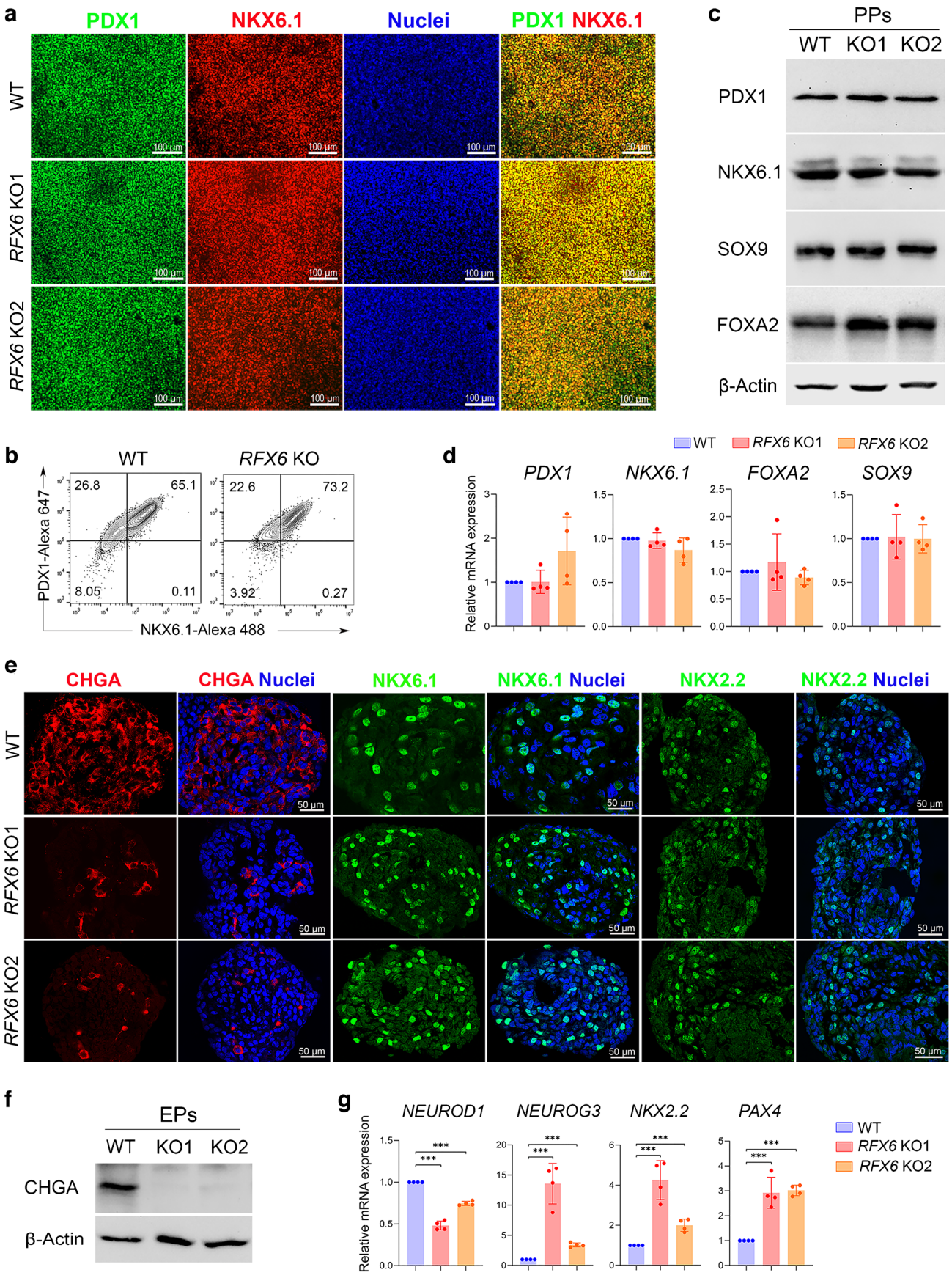
a
PDX1
NKX6.1
Nuclei
PDX1 NKX6.1
WT
RFX6 KO1
RFX6 KO2
100 μm
c
PPs
WT KO1 KO2
PDX1
NKX6.1
SOX9
FOXA2
β-Actin
b
WT
RFX6 KO
26.8
65.1
8.05
0.11
22.6
73.2
3.92
0.27
PDX1-Alexa 647
NKX6.1-Alexa 488
d
WT
RFX6 KO1
RFX6 KO2
PDX1
NKX6.1
FOXA2
SOX9
Relative mRNA expression
e
CHGA
CHGA Nuclei
NKX6.1
NKX6.1 Nuclei
NKX2.2
NKX2.2 Nuclei
WT
RFX6 KO1
RFX6 KO2
50 μm
f
EPs
WT KO1 KO2
CHGA
β-Actin
g
NEUROD1
NEUROG3
NKX2.2
PAX4
Relative mRNA expression
***
WT
RFX6 KO1
RFX6 KO2

◂**Fig. 3** Impact of *RFX6* depletion on the expression of crucial pancreatic progenitor and endocrine progenitor markers. (**a**, **b**) Immunofluorescence staining (**a**) and flow cytometry analysis (**b**) showing the co-expression of PDX1 and NKX6.1 in PPs derived from WT iPSCs and *RFX6* KO iPSCs. $PDX1^+/NKX6.1^+$ cells are shown in the upper right quadrant in (**b**). (**c**) Western blot analysis showing the protein expression of PDX1, NKX6.1, SOX9 and FOXA2 in *RFX6* KO PPs compared with WT PPs. (**d**) RT-qPCR analysis showing the mRNA expression of PP markers *PDX1*, *NKX6.1*, *FOXA2* and *SOX9* in *RFX6* KO PPs relative to WT PPs (n=4). (**e**) Immunofluorescence staining showing the expression of CHGA, NKX6.1 and NKX2.2 in EPs derived from WT iPSCs and *RFX6* KO iPSCs. (**f**) Western blot analysis showing the expression of CHGA in *RFX6* KO EPs compared with WT EPs. (**g**) RT-qPCR analysis showing the mRNA expression of EP markers *NEUROD1*, *NEUROG3*, *NKX2.2* and *PAX4* in *RFX6* KO EPs relative to WT EPs (n=4). The data are presented as mean ± SD. ***p<0.001. Scale bar, 50 µm (**e**) or 100 µm (**a**)

PTPRN, *PRPRN2*, *FEV* and *LMX1B* in *RFX6* KO PPs compared with WT PPs (Fig. 4d, Table 1). Furthermore, at the EP stage, the RT-qPCR revealed significant decrease in the expression of endocrine genes including *ARX*, *PAX6*, *ISL1*, *IRX2*, *INS*, *GCG*, *SST*, *NEUROD1*, *PCSK1*, *SCGN*, *ERO1B*, *MAFB*, *SIX3*, *KCTD12* and *LMX1B* in *RFX6* KO EPs compared with WT EPs (Fig. 4e; Table 1).

***RFX6* loss correlates with the generation of smaller pancreatic islet organoids** To enhance islet differentiation after stage 4, cells were cultured in suspension to form organoids, with an equal number of WT PP and KO PP cells used. Although during the first 2 days of stage 5 no notable difference between WT and KO organoids was observed, a significant variation in organoid size became evident as differentiation progressed. Islet organoids derived from *RFX6* KO iPSCs showed smaller size and irregular shapes compared with those derived from WT iPSCs during stages 5 and 6 (Fig. 5a and ESM Fig. 6a).

To investigate whether the dramatic reduction in islet organoid size could be attributed to either cell death or inhibition of cell proliferation, we conducted apoptosis and proliferation assays during stage 5 of differentiation. Flow cytometry analysis demonstrated a significant increase in the proportion of Annexin V^+ cells in *RFX6* KO EPs compared with WT EPs (Fig. 5b). Although increased apoptosis was also observed in the final stage of differentiation (stage 6), its level was lower compared with EPs (ESM Fig. 6b), indicating increased cell death with its peak during the EP stage. Quantification of BrdU incorporation revealed no significant difference in proliferation rates between WT and KO cells (Fig. 5c), suggesting that reduced islet organoid size due to *RFX6* loss mainly results from increased cell death.

To elucidate the mechanism underlying the increased cell death, we analysed the top DEGs identified from our RNA-seq data. Interestingly, we observed a significant downregulation of *CAT* (encoding for catalase [CAT], an antioxidant enzyme that is known to protect cells against oxidative stress [31]) in both *RFX6* KO PPs ($\log_2$ fold change = −7.459; $p=9.62\times10^{-35}$) and *RFX6* KO EPs ($\log_2$ fold change = −6.978; $p=1.87\times10^{-26}$) compared with WT controls (Fig. 5d). This finding was validated at the protein level through western blot and immunostaining analyses, revealing an almost complete absence of CAT expression in both *RFX6* KO PPs and *RFX6* KO EPs compared with their respective controls (Fig. 5e, f). To validate the role of the CAT in promoting cell survival, we employed the STRING tool for protein functional interaction prediction [27]. Our analysis revealed CAT's strong interaction with antioxidative stress proteins, such as superoxide dismutase proteins (ESM Fig. 6c).

***RFX6* loss hinders the development of pancreatic islet cells** Subsequent differentiation into pancreatic islets demonstrated a lack of expression for INS, proinsulin, GCG, SST and urocortin 3 (UCN3), alongside a significant decrease in CHGA in *RFX6* KO islets compared with WT islets (Fig. 6a, b). This indicates that *RFX6* is essential for the formation of alpha, beta and delta cells. These reductions were confirmed at the mRNA level for *INS*, *GCG*, *SST* and *UCN3* (Fig. 6c). Furthermore, other key pancreatic islet markers, including *IAPP*, *PAX6*, *ARX*, *GCK*, *MAFA*, *KCNJ11*, *ABCC8*, *SLC18A1* and *FEV*, were significantly downregulated (Fig. 6c). On the other hand, pancreatic polypeptide Y (PPY) was significantly upregulated at mRNA and protein levels (Fig. 6c and ESM Fig. 6d). In response to various glucose concentrations, *RFX6* KO islets exhibited no significant changes in INS secretion, with their total INS content being significantly lower than that in WT controls (ESM Fig. 6e).

RFX6 overexpression rescues the expression of dysregulated genes in pancreatic cells lacking *RFX6* Next, we aimed to reverse RFX6-associated defects by ectopically expressing *RFX6* (*RFX6* overexpression [OE]). *RFX6* was overexpressed on days 2 and 4 of stage 4 for assessing its effect on PPs and EPs, and subsequently on islets (Fig. 7). At the end of stage 4, the *RFX6* OE significantly increased mRNA expression levels of pancreatic endocrine genes that were downregulated in *RFX6* KO PPs, including *RFX6*, *ARX*, *PAX6*, *CHGA*, *IRX1*, *IRX2*, *INS*, *GCG*, *SST*, *MAFB*,

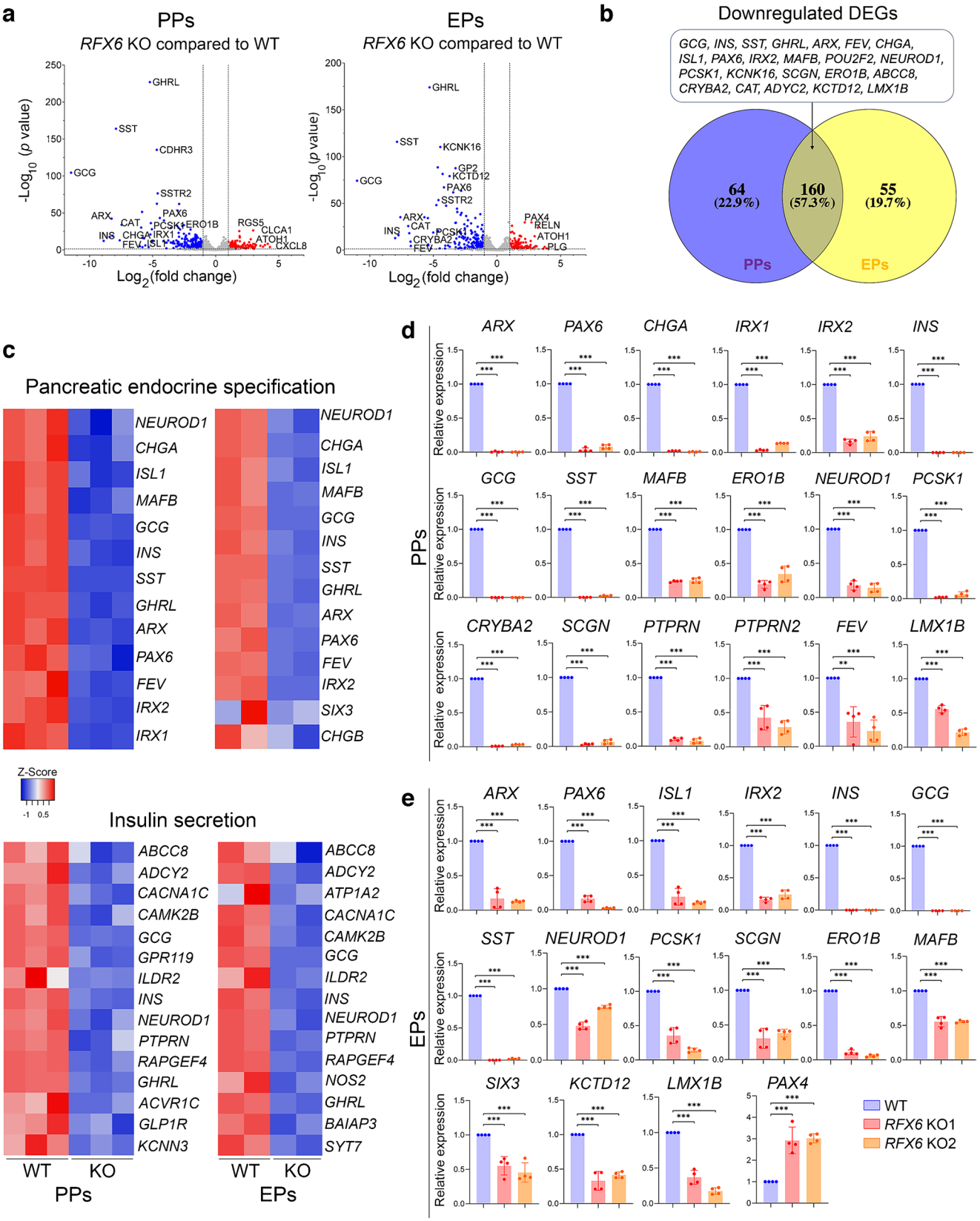
a
PPs
RFX6 KO compared to WT
EPs
RFX6 KO compared to WT
-Log10 (p value)
Log2(fold change)
GHRL
SST
CDHR3
GCG
SSTR2
ARX
PAX6
CAT
PCSK1
ERO1B
INS
CHGA
IRX1
FEV
ISL1
RGS5
CLCA1
ATOH1
CXCL8
KCNK16
GP2
KCTD12
PAX6
SSTR2
CRYBA2
PAX4
RELN
PLG
b
Downregulated DEGs
GCG, INS, SST, GHRL, ARX, FEV, CHGA, ISL1, PAX6, IRX2, MAFB, POU2F2, NEUROD1, PCSK1, KCNK16, SCGN, ERO1B, ABCC8, CRYBA2, CAT, ADYC2, KCTD12, LMX1B
64 (22.9%)
160 (57.3%)
55 (19.7%)
PPs
EPs
c
Pancreatic endocrine specification
NEUROD1
CHGA
ISL1
MAFB
GCG
INS
SST
GHRL
ARX
PAX6
FEV
IRX2
IRX1
SIX3
CHGB
Z-Score
Insulin secretion
ABCC8
ADCY2
CACNA1C
CAMK2B
GCG
GPR119
ILDR2
INS
NEUROD1
PTPRN
RAPGEF4
GHRL
ACVR1C
GLP1R
KCNN3
ATP1A2
NOS2
BAIAP3
SYT7
WT
KO
PPs
EPs
d
ARX
PAX6
CHGA
IRX1
IRX2
INS
GCG
SST
MAFB
ERO1B
NEUROD1
PCSK1
CRYBA2
SCGN
PTPRN
PTPRN2
FEV
LMX1B
Relative expression
PPs
e
ARX
PAX6
ISL1
IRX2
INS
GCG
SST
NEUROD1
PCSK1
SCGN
ERO1B
MAFB
SIX3
KCTD12
LMX1B
PAX4
Relative expression
EPs
WT
RFX6 KO1
RFX6 KO2

◀**Fig. 4** Impact of *RFX6* loss on transcriptomic profiles of iPSC-derived PPs and EPs. Bulk RNA-seq analysis was performed on PPs (n=3) and EPs (n=2) derived from *RFX6* KO iPSCs and WT iPSCs. (**a**) Volcano plots display the DEGs in *RFX6* KO PPs and *RFX6* KO EPs compared with their WT controls. Downregulated genes are represented by blue dots, while upregulated genes are depicted by red dots. (**b**) Venn diagram illustrating the intersection of downregulated DEGs in *RFX6* KO PPs and *RFX6* KO EPs. Note that most of those DEGs are endocrine pancreatic genes. (**c**) Heatmap of z score value of pancreatic endocrine and INS secretion genes downregulated in *RFX6* KO PPs and *RFX6* KO EPs compared with WT PPs and WT EPs, respectively. (**d**, **e**) RT-qPCR validation of the DEGs in PPs (**d**) and EPs (**e**) derived from two different KO iPSC lines (n=4). The data are presented as mean ± SD. **p<0.01, ***p<0.001

ERO1B, *NEUROD1*, *PCSK1*, *ISL1*, *CRYBA2*, *SCGN*, *PTPRN*, *PTPRN2* and *LMX1B* (Fig. 7a). Furthermore, we assessed the impact of *RFX6* OE on the dysregulated DEGs on day 3 of stage 5, 72 h post-transfection. Our results revealed a substantial increase in the expression levels of *INS*, *GCG*, *SST*, *NEUROD1*, *CHGA*, *CHGB*, *PAX6*, *ARX*, *ISL1*, *MAFB*, *PCSK1*, *ERO1B*, *IRX2*, *CRYBA2*, *KCTD12*, *LMX1B*, *SCGN* and *SSTR2* following *RFX6* OE (Fig. 7b). Moreover, it induced a significant decrease in the *PAX4* mRNA levels, which had been upregulated in *RFX6* KO EPs (Fig. 7b). In addition, *RFX6* OE at the end of stage

Table 1 Key downregulated DEGs associated with pancreatic endocrine development and function in PPs and EPs lacking *RFX6* ($\log_2$ fold change < –1, p<0.05)

PPs			EPs		
Gene	$\log_2$ FC	p value	Gene ID	$\log_2$ FC	p value
GCG	−11.470	3.56×10^{-105}	*GCG*	−11.002	6.40×10^{-75}
INS	−8.409	2.04×10^{-18}	*INS*	−7.747	1.05×10^{-16}
SST	−7.909	1.29×10^{-164}	*SST*	−7.860	1.42×10^{-116}
GHRL	−5.224	1.00×10^{-227}	*GHRL*	−5.303	8.81×10^{-175}
ARX	−8.255	4.47×10^{-43}	*ARX*	−7.600	5.66×10^{-36}
CHGA	−5.818	4.65×10^{-17}	*CHGA*	−6.103	0.00
ISL1	−5.681	2.47×10^{-16}	*ISL1*	−5.418	9.30×10^{-7}
PAX6	−4.434	6.02×10^{-44}	*PAX6*	−4.172	6.96×10^{-68}
MAFB	−2.653	4.23×10^{-33}	*MAFB*	−2.863	1.70×10^{-38}
NEUROD1	−2.944	1.97×10^{-11}	*NEUROD1*	−3.148	4.23×10^{-45}
FEV	−7.615	1.13×10^{-13}	*FEV*	−6.774	3.32×10^{-5}
IRX2	−3.056	3.41×10^{-33}	*IRX2*	−2.881	1.92×10^{-20}
IRX1	−5.180	1.25×10^{-21}	*SIX3*	−1.056	2.26×10^{-2}
ABCC8	−1.908	1.26×10^{-6}	*ABCC8*	−1.540	5.13×10^{-4}
ADCY2	−2.396	1.37×10^{-10}	*ADCY2*	−2.238	4.23×10^{-9}
CACNA1C	−2.398	3.72×10^{-18}	*CACNA1C*	−2.100	2.73×10^{-12}
CAMK2B	−2.335	7.84×10^{-11}	*CAMK2B*	−2.689	2.18×10^{-15}
ILDR2	−2.268	2.90×10^{-8}	*ILDR2*	−2.602	2.67×10^{-14}
PTPRN	−2.724	3.36×10^{-6}	*PTPRN*	−3.444	1.58×10^{-62}
RAPGEF4	−1.470	5.63×10^{-18}	*RAPGEF4*	−1.558	3.86×10^{-13}
ACVR1C	−1.778	1.46×10^{-6}	*NOS2*	−4.068	1.53×10^{-05}
GLP1R	−1.185	6.04×10^{-7}	*BAIAP3*	−1.497	1.76×10^{-16}
GPR119	−5.318	1.72×10^{-4}	*ATP1A2*	−2.165	2.18×10^{-4}
CACNA1C	−2.398	3.72×10^{-18}	*CACNA1C*	−2.100	2.73×10^{-12}
CACNA2D1	−2.013	2.16×10^{-12}	*CACNA2D1*	−2.294	9.37×10^{-33}
CACNG7	−1.268	3.05×10^{-2}	*CACNG7*	−1.889	2.50×10^{-4}
CACNA1A	−1.864	1.70×10^{-12}	*CACNA1A*	−2.001	2.16×10^{-18}
CACNA1B	−1.351	6.87×10^{-7}	*CACNA1B*	−1.460	8.02×10^{-7}
KCNJ6	−2.440	1.96×10^{-10}	*KCNJ6*	−2.626	6.00×10^{-13}
KCNK16	−3.887	1.24×10^{-10}	*KCNK16*	−4.462	5.35×10^{-111}
KCNK17	−1.774	4.11×10^{-8}	*KCNK17*	−1.698	2.93×10^{-17}
KCNC4	−1.415	2.00×10^{-6}	*KCNC4*	−1.528	5.24×10^{-5}
KCND3	−1.548	1.05×10^{-15}	*KCND3*	−1.654	2.84×10^{-12}
KCNH6	−1.414	1.63×10^{-2}	*KCNH6*	−2.025	3.05×10^{-21}
SCN3A	−1.766	7.56×10^{-7}	*SCN3A*	−2.292	6.99×10^{-14}
SCN7A	−1.370	4.49×10^{-6}	*KCNV1*	−1.018	3.60×10^{-5}
KCNN3	−2.817	9.59×10^{-9}	*SYT7*	−1.192	1.52×10^{-14}
KCNJ5	−3.003	4.47×10^{-12}	*CHGB*	−1.212	6.04×10^{-5}
KCNK10	−2.476	8.32×10^{-6}			

FC, fold change

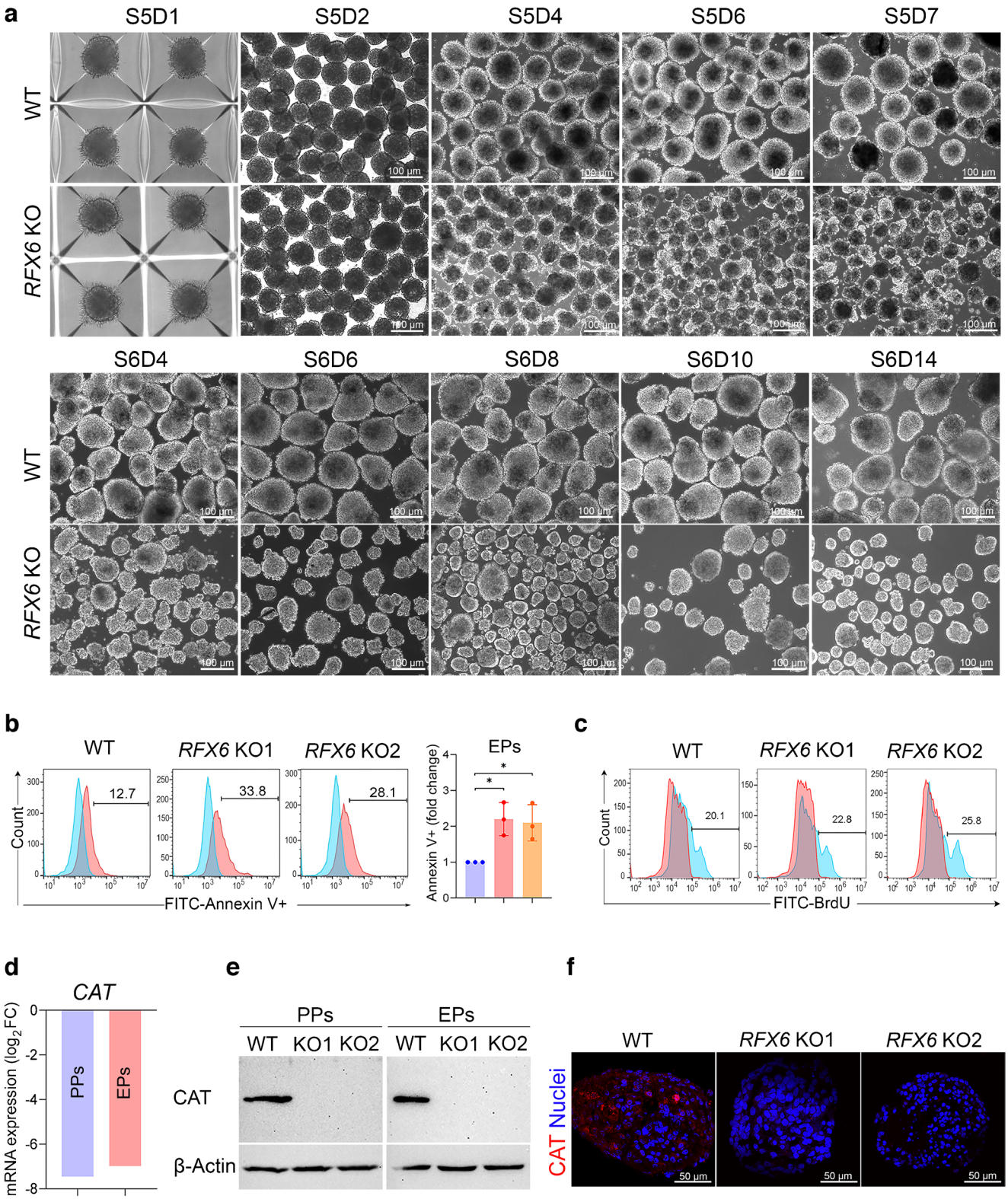
a
S5D1
S5D2
S5D4
S5D6
S5D7
WT
RFX6 KO
100 μm
S6D4
S6D6
S6D8
S6D10
S6D14
b
WT
RFX6 KO1
RFX6 KO2
12.7
33.8
28.1
Count
FITC-Annexin V+
EPs
Annexin V+ (fold change)
c
20.1
22.8
25.8
FITC-BrdU
d
CAT
mRNA expression (log2FC)
PPs
EPs
e
PPs
EPs
WT KO1 KO2 WT KO1 KO2
CAT
β-Actin
f
CAT Nuclei
50 μm

◂**Fig. 5** Influence of *RFX6* deletion on pancreatic islet organoid formation and cell viability. (**a**) Comparative morphological analysis of pancreatic islet organoids derived from two *RFX6* KO iPSC lines vs WT iPSCs during differentiation stages 5 and 6 (n=3); S, stage, D, day. (**b**) Representative flow cytometry analysis and quantification of apoptosis (Annexin V^+ cells) on day 3 of stage 5 of differentiation indicates a significant increase in apoptosis in *RFX6* KO EPs in comparison with WT EPs (n=3). (**c**) Flow cytometry analysis of BrdU incorporation reveals a slight increase in cell proliferation ($BrdU^+$ cells) in EPs derived from *RFX6* KO iPSC lines compared with those derived from WT iPSCs. (**d**) Log_2 fold change in the expression of *CAT* mRNA in *RFX6* KO PPs and *RFX6* KO EPs compared with WT controls, based on RNA-seq data analysis. (**e**) Western blot analysis showing the absence of CAT protein in *RFX6* KO PPs and *RFX6* KO EPs compared with WT controls. (**f**) Immunofluorescence images showing the lack of CAT expression in *RFX6* KO EPs compared with WT EPs. The data are presented as mean ± SD. *p<0.05; (**d**) PPs $p=9.62 \times 10^{-35}$; EPs $p=1.87 \times 10^{-26}$. Scale bar, 50 µm (**f**) or 100 µm (**a**)

4 increased the expression of INS, GCG and SST in the *RFX6* KO islets (Fig. 7c).

Discussion

Recent studies have highlighted the pivotal role of RFX6 in human pancreatic islet development and function, and its association with diabetes [3, 28, 32, 33]. Nonetheless, its exact role in diabetes pathogenesis is still poorly understood and a comprehensive understanding of its specific function during human pancreatic islet development is needed. In this study, we precisely examined RFX6 expression across different stages of hPSC-derived pancreatic islets using different approaches. Furthermore, we developed an isogenic KO platform using human iPSC-derived islets to investigate molecular and cellular alterations at different developmental stages carrying *RFX6* loss-of-function mutations. Our findings are consistent with previous studies, showing the following results: (1) the absence of INS-, GCG- and SST-producing cells and an increase in PPY cell production due to *RFX6* loss; and (2) significant downregulation of genes related to pancreatic endocrine differentiation, INS secretion and ion transport in association with *RFX6* loss [4, 32, 33]. In addition, our study unveils novel insights into the role of RFX6 during pancreatic islet development. Our data indicate the absence of RFX6 does not impede iPSC differentiation into PPs co-expressing PDX1 and NKX6.1, which serve as precursors to pancreatic beta cells. Furthermore, RFX6 deficiency results in the formation of smaller-sized (hypoplastic) islet organoids, potentially driven by increased cellular apoptosis and likely linked to the deficiency of the antioxidant enzyme CAT. These findings imply that pancreatic hypoplasia and the absence of islet cells due to *RFX6* loss-of-function mutations are associated with cellular apoptosis, reduced CAT enzyme expression and reduced pancreatic endocrine gene expression.

Our findings revealed a significant decrease in PDX1 and CDX2 expression in *RFX6* KO PF compared with WT PF, consistent with recent findings [33, 34]. However, the absence of RFX6 did not impact the co-expression of PDX1 and NKX6.1 in PPs. These results align with our timeline expression analysis, which demonstrated the co-localisation of RFX6 with PDX1 in the PF stage, while RFX6 showed no co-expression with PDX1 and NKX6.1 in PPs. The difference in the impact on PDX1 expression between PF and PP stages observed in this study may be attributed to RFX6's involvement during early differentiation stages in intestinal development, as recently reported in iPSC-derived intestinal models [35]. RFX6 plays a crucial role in both pancreas and small-intestine development, as these organs share a common origin in the gut endoderm [34]. PDX1, crucial for pancreas development, also influences small-intestine development and function. Previous studies suggest that PDX1 acts downstream of RFX6 during gut-tube patterning, with co-expression in EECs of the duodenum and iPSC-derived gut endoderm [35–37]. *RFX6* mutant iPSCs generated defective intestinal organoids due to suppression of PDX1 expression [35]. Our results contradict those of two prior studies. One demonstrated a significant decrease in PDX1 and NKX6.1 levels in PPs derived from MRS patient-specific iPSCs and *RFX6* KO iPSCs [28]. The other study, utilising *RFX6* KO-hESCs, indicated a reduction in the number of PPs due to a marked decrease in PDX1 expression [32]. Our findings suggest that inhibition of PDX1 expression associated with *RFX6* loss prior to the PP stage may disrupt intestinal development, supported by a significant reduction in CDX2 expression, crucial for intestinal development [38]. Furthermore, RFX6 is not essential for forming $PDX1^+/NKX6.1^+$ PPs during pancreatic islet development.

The deficiency of RFX6 led to impaired expression of critical transcription factors and genes essential for endocrine cell development across various stages, including *PAX6*, *INSM1*, *ARX*, *NEUROD1*, *ISL1*, *IRX1*, *IRX2*, *MAFB*, *TTR*, *FEV* and *CHGA* among others. Conversely, the expression of transcription factors such as

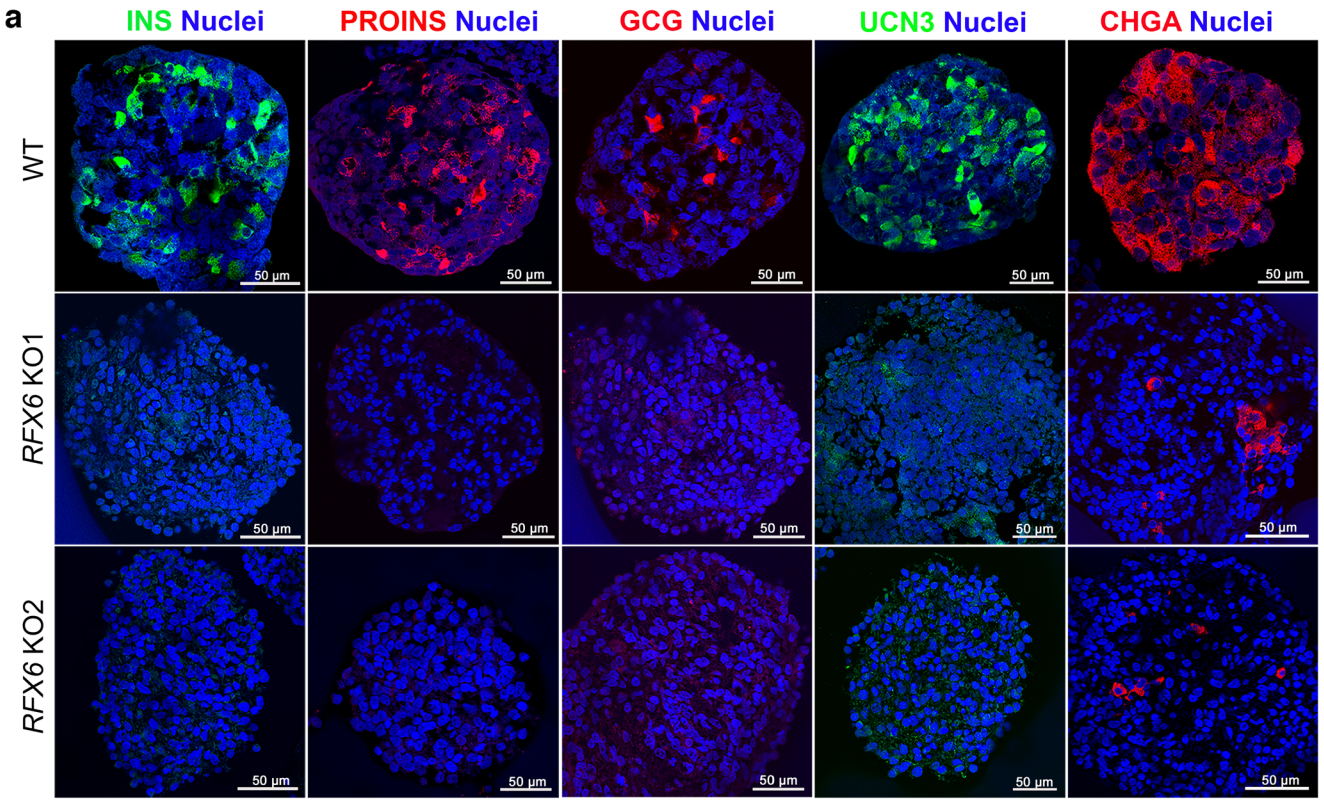
a
INS Nuclei
PROINS Nuclei
GCG Nuclei
UCN3 Nuclei
CHGA Nuclei
WT
RFX6 KO1
RFX6 KO2
50 μm

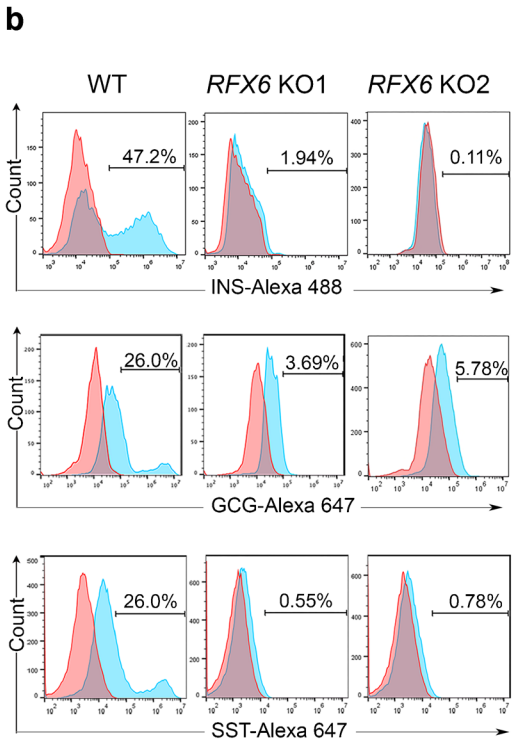
b
WT
RFX6 KO1
RFX6 KO2
Count
47.2%
1.94%
0.11%
INS-Alexa 488
26.0%
3.69%
5.78%
GCG-Alexa 647
26.0%
0.55%
0.78%
SST-Alexa 647

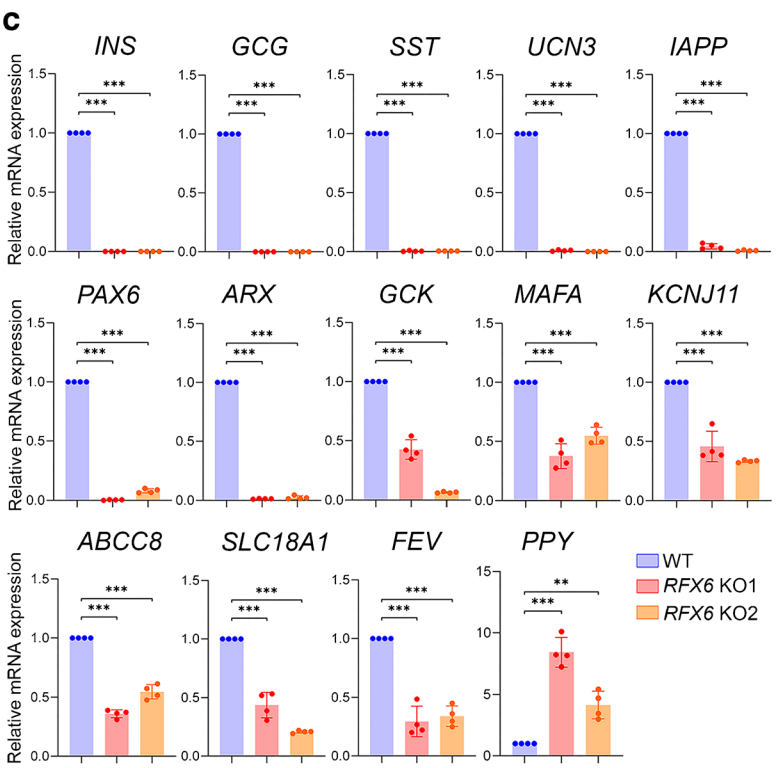
c
INS
GCG
SST
UCN3
IAPP
PAX6
ARX
GCK
MAFA
KCNJ11
ABCC8
SLC18A1
FEV
PPY
Relative mRNA expression
WT
RFX6 KO1
RFX6 KO2

◂**Fig. 6** *RFX6* loss impairs the development of pancreatic islet cells. (**a**) Confocal immunofluorescence showing expression of pancreatic islet markers INS, proinsulin (PROINS), GCG, UCN3 and CHGA in islets derived from two different *RFX6* KO iPSC lines compared with WT controls (n=3). (**b**) Flow cytometry analysis of the expression of INS, GCG and SST in islets derived from *RFX6* KO iPSCs compared with expression in islets derived from WT iPSCs (n=3). (**c**) RT-qPCR analysis for the mRNA expression of key islet genes *INS*, *GCG*, *SST*, *UCN3*, *IAPP*, *PAX6*, *ARX*, *GCK*, *MAFA*, *KCNJ11*, *ABCC8*, *SCL18A1*, *FEV* and *PPY* (n=4). Data are represented as mean ± SD; **p<0.01, ***p<0.001. Scale bar, 50 μm

PDX1, NKX6.1, SOX9 and FOXA2, specific to PPs [39], remained unaffected by the absence of RFX6 in the PPs, while endocrine transcription factors such as paired box 4 (PAX4), NEUROG3 and NKX2.2 were increased in the EPs due to RFX6 deficiency. These findings are consistent with recent results indicating that *RFX6* loss does not affect SOX9 expression and increases the expression of NEUROG3, PAX4 and NKX2.2 [33]. RFX6 acts downstream of NEUROG3 during pancreatic development [1], regulating PAX4 expression [40]. Our re-analysis of single-cell data obtained from different stages of hESC differentiation into pancreatic islets [25] confirmed the highest *RFX6* expression levels in endocrine clusters, including *NEUROG3*^{high}/*GHRL*^{high}, CHGA^{high}/*NEUROD1*^{high}, *ERO1LB*^{high}/*ARX*^{high}, *POU2F2*^{high}/*RFX3*^{high}, *TTR*^{high}/*GCG*^{high}, *GCG*^{high}/*CHGA*^{high} and *HHEX*^{high}/*SST*^{high}. The analysis revealed that clusters with high PDX1 and SOX9 expression during the progenitor stages (D11 and D14) did not exhibit RFX6 expression. A recent report highlighted a developmental trajectory emerging at stage 4 (PPs), leading to the formation of primary endocrine cell groups. The differentiation process becomes notably intricate during stage 5 (EPs), primarily due to the presence of numerous subpopulations [40]. A recent study emphasised RFX6's role in alpha cell function, revealing that its absence leads to impaired exocytosis and GCG secretion, complementing previous findings on beta cell development [41]. These findings underscore the crucial role of RFX6 in regulating pancreatic endocrine genes important for islet cell development, including *GCG* (alpha cells), *INS* (beta cells) and *SST* (delta cells).

Biallelic mutations in *RFX6* are associated with permanent neonatal diabetes mellitus (PNDM), with affected individuals exhibiting smaller size pancreas compared with healthy control individuals [4]. The cause of this pancreatic hypoplasia remains unclear. Recent human studies have suggested that reduced pancreas size may result from suppressed PDX1 expression at the PP stage [28, 32]. However, our current study demonstrated *RFX6* deletion reduced PDX1 in PF without affecting its expression at the PP stage, suggesting other mechanisms. Islet organoids derived from *RFX6* KO iPSCs were smaller in size compared with WT controls due to increased apoptosis during endocrine specification stages. This contradicts a previous *RFX6* KO hESC study suggesting reduced pancreas size is not caused by reduced proliferation or increased apoptosis but from the reduction in PDX1 at early stages of pancreatic development [32]. In our endeavour to unravel the mechanism behind increased cell death in pancreatic cells lacking *RFX6*, our RNA-seq analysis identified antioxidant enzyme CAT downregulation as a potential cause for the increased cell death. Western blotting and immunostaining confirmed the absence of CAT in *RFX6* KO PPs and *RFX6* KO EPs vs WT control PPs and EPs. CAT regulates cellular hydrogen peroxide levels, safeguarding beta cells against oxidative damage [42, 43]. Elevated hydrogen peroxide levels can harm pancreatic beta cells and disrupt INS production [42, 44]. Mutations in *CAT* , elevating hydrogen peroxide, may increase type 2 diabetes risk due to peroxide-induced beta cell damage [45]. Taken together, these findings indicate that RFX6 plays a crucial role in safeguarding pancreatic islets during development by maintaining CAT expression, thereby offering protection against oxidative damage.

In summary, our study explored the effects of *RFX6* deletion on pancreatic islet development. It showed a substantial reduction in PDX1 expression in *RFX6* KO PF, consistent with earlier studies. However, the absence of RFX6 did not disrupt the development of PDX1 and NKX6.1 in PPs, aligning with the lack of RFX6 co-expression with key progenitor markers and its absence in cell clusters expressing high levels of PDX1 and SOX9 in PPs. RFX6's role in early intestinal development may explain the PDX1 expression differences between PFs and PPs. Furthermore, our findings indicate that RFX6 regulates the expression of crucial pancreatic endocrine genes essential for the formation of INS-, GCG- and SST-expressing cells during pancreatic differentiation. Moreover, *RFX6* deletion resulted in smaller islet organoids, attributed to increased cell apoptosis during endocrine specification. These results underscore RFX6's pivotal role in safeguarding pancreatic islets, potentially explaining pancreatic hypoplasia in individuals with *RFX6* homozygous mutations. Thus, our study highlights

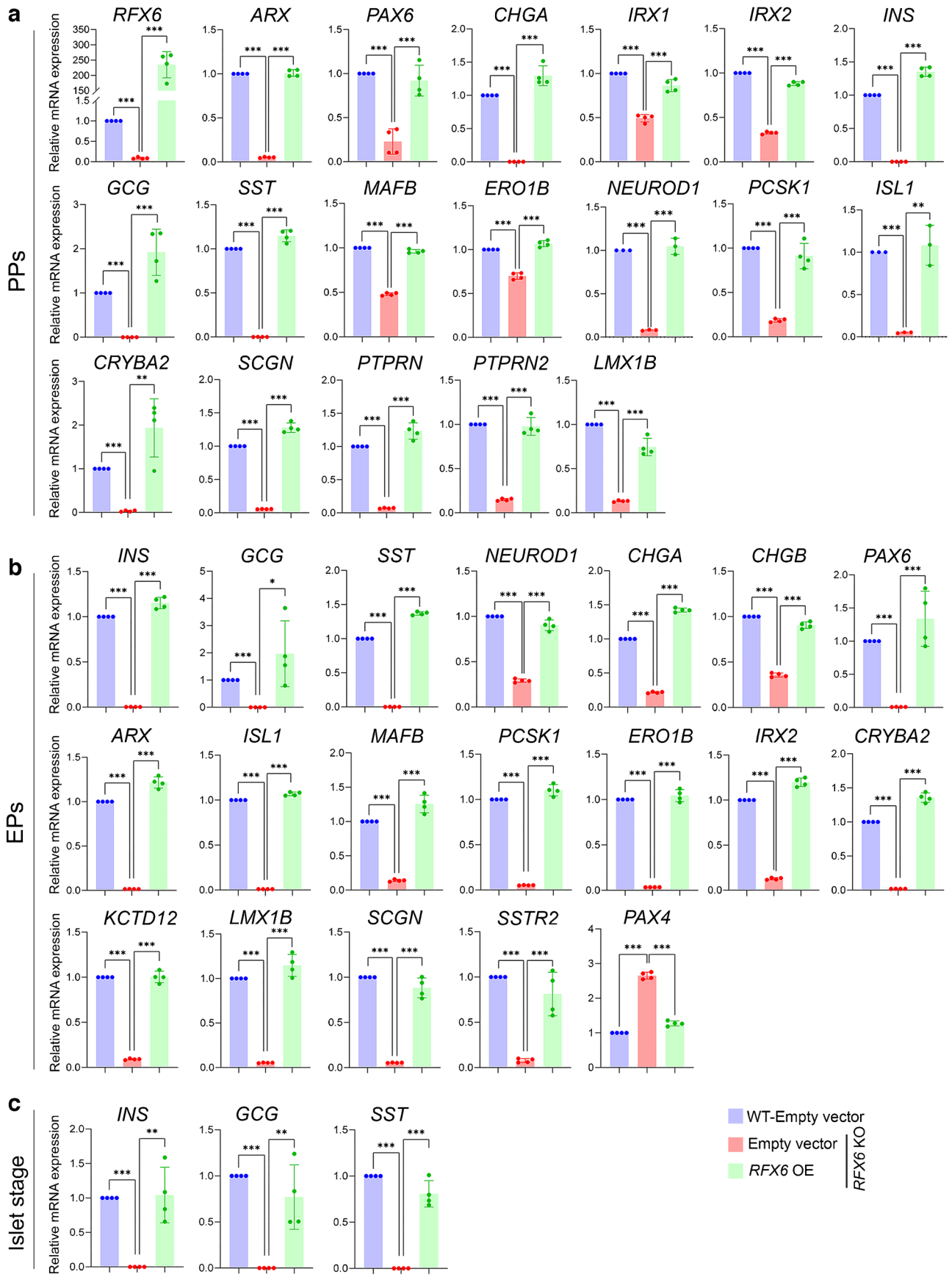
a
PPs
RFX6
ARX
PAX6
CHGA
IRX1
IRX2
INS
GCG
SST
MAFB
ERO1B
NEUROD1
PCSK1
ISL1
CRYBA2
SCGN
PTPRN
PTPRN2
LMX1B
b
EPs
INS
GCG
SST
NEUROD1
CHGA
CHGB
PAX6
ARX
ISL1
MAFB
PCSK1
ERO1B
IRX2
CRYBA2
KCTD12
LMX1B
SCGN
SSTR2
PAX4
c
Islet stage
INS
GCG
SST
Relative mRNA expression
WT-Empty vector
Empty vector
RFX6 OE
RFX6 KO

◂**Fig. 7** RFX6 overexpression rescues the expression of dysregulated genes in pancreatic cells lacking *RFX6*. (**a**) RT-qPCR analysis for the expression of pancreatic endocrine genes: *RFX6*, *ARX*, *PAX6*, *CHGA*, *IRX1*, *IRX2*, *INS*, *GCG*, *SST*, *MAFB*, *ERO1B*, *NEUROD1*, *PCSK1*, *ISL1*, *CRYBA2*, *SCGN*, *PTPRN*, *PTPRN2* and *LMX1B* in PPs derived from *RFX6* KO iPSCs and WT iPSCs, 48 h following ectopic expression of RFX6 (n=4). (**b**) RT-qPCR analysis for the expression of pancreatic endocrine genes: *INS*, *GCG*, *SST*, *NEUROD1*, *CHGA*, *CHGB*, *PAX6*, *ARX*, *ISL1*, *MAFB*, *PCSK1*, *ERO1B*, *IRX2*, *CRYBA2*, *KCTD12*, *LMX1B*, *SCGN*, *SSTR2* and *PAX4*, in EPs derived from *RFX6* KO iPSCs and WT iPSCs, 72 h following ectopic expression of RFX6 (n=4). (**c**) RT-qPCR analysis for the expression of *INS*, *GCG* and *SST* in islet organoids at stage 6 following overexpression of RFX6 at the end of stage 4 (n=4). Data are represented as mean ± SD; *p<0.05, **p<0.01, ***p<0.001

the complexity of RFX6's role in pancreatic islet development and its implications for understanding pancreatic hypoplasia and diabetes risk.

Supplementary Information The online version of this article (https://doi.org/10.1007/s00125-024-06232-2) contains peer-reviewed but unedited supplementary material.

Acknowledgements We would like to thank N. R. Dunn (A*STAR, Singapore) for providing the HA-RFX6 tagged H9 hESC lines (*RFX6*$^{HA/HA}$ H9-hESCs). Furthermore, we thank the Genomic Core members at QBRI for their assistance with technical support in RNA-seq.

Data availability RNA-seq datasets have been deposited in the Zenodo repository with accession link (DOI: https://doi.org/10.5281/zenodo.10656891).

Funding Open Access funding provided by the Qatar National Library. This work was funded by grants from Qatar Biomedical Research Institute (QBRI) (Grant no. QBRI-HSCI Project 1). NA is a PhD student with a scholarship funded by QRDI (GSRA9-L-1-0511-22008).

Authors' relationships and activities SH is a co-founder and shareholder of Sequantrix GmbH and has research funding from Novo Nordisk and Askbio. The authors declare that there are no other relationships or activities that might bias, or be perceived to bias, their work.

Contribution statement NA performed most of the experiments and analysed the data. AKE and BM performed experiments and analysed the data. SI and SH analysed the sequencing data. EMA conceived and designed the study, supervised the project, analysed and interpreted the data, and wrote the manuscript. All authors critically reviewed the article and approved the final version of the manuscript. EMA is the guarantor of this work.

References

1. Smith SB, Qu HQ, Taleb N et al (2010) Rfx6 directs islet formation and insulin production in mice and humans. Nature 463(7282):775–780. https://doi.org/10.1038/nature08748
2. Concepcion JP, Reh CS, Daniels M et al (2014) Neonatal diabetes, gallbladder agenesis, duodenal atresia, and intestinal malrotation caused by a novel homozygous mutation in RFX6. Pediatr Diabetes 15(1):67–72. https://doi.org/10.1111/pedi.12063
3. Sansbury FH, Kirel B, Caswell R et al (2015) Biallelic RFX6 mutations can cause childhood as well as neonatal onset diabetes mellitus. Eur J Hum Genet 23(12):1744–1748. https://doi.org/10.1038/ejhg.2015.161
4. Chandra V, Albagli-Curiel O, Hastoy B et al (2014) RFX6 regulates insulin secretion by modulating Ca2+ homeostasis in human beta cells. Cell Rep 9(6):2206–2218. https://doi.org/10.1016/j.celrep.2014.11.010
5. Mitchell J, Punthakee Z, Lo B et al (2004) Neonatal diabetes, with hypoplastic pancreas, intestinal atresia and gall bladder hypoplasia: search for the aetiology of a new autosomal recessive syndrome. Diabetologia 47(12):2160–2167. https://doi.org/10.1007/s00125-004-1576-3
6. Pearl EJ, Jarikji Z, Horb ME (2011) Functional analysis of Rfx6 and mutant variants associated with neonatal diabetes. Dev Biol 351(1):135–145. https://doi.org/10.1016/j.ydbio.2010.12.043
7. Patel KA, Kettunen J, Laakso M et al (2017) Heterozygous RFX6 protein truncating variants are associated with MODY with reduced penetrance. Nat Commun 8(1):888. https://doi.org/10.1038/s41467-017-00895-9
8. Mohan V, Radha V, Nguyen TT et al (2018) Comprehensive genomic analysis identifies pathogenic variants in maturity-onset diabetes of the young (MODY) patients in South India. BMC Med Genet 19(1):22. https://doi.org/10.1186/s12881-018-0528-6
9. Imaki S, Iizuka K, Horikawa Y et al (2021) A novel RFX6 heterozygous mutation (p.R652X) in maturity-onset diabetes mellitus: A case report. J Diabetes Investig 12(10):1914–1918. https://doi.org/10.1111/jdi.13545
10. Piccand J, Strasser P, Hodson DJ et al (2014) Rfx6 maintains the functional identity of adult pancreatic beta cells. Cell Rep 9(6):2219–2232. https://doi.org/10.1016/j.celrep.2014.11.033
11. Ray D, Chatterjee N (2020) A powerful method for pleiotropic analysis under composite null hypothesis identifies novel shared loci between Type 2 Diabetes and Prostate Cancer. PLoS Genet 16(12):e1009218. https://doi.org/10.1371/journal.pgen.1009218
12. Varshney A, Scott LJ, Welch RP et al (2017) Genetic regulatory signatures underlying islet gene expression and type 2 diabetes. Proc Natl Acad Sci U S A 114(9):2301–2306. https://doi.org/10.1073/pnas.1621192114
13. Soyer J, Flasse L, Raffelsberger W et al (2010) Rfx6 is an Ngn3-dependent winged helix transcription factor required for pancreatic islet cell development. Development 137(2):203–212. https://doi.org/10.1242/dev.041673
14. Spiegel R, Dobbie A, Hartman C, de Vries L, Ellard S, Shalev SA (2011) Clinical characterization of a newly described neonatal diabetes syndrome caused by RFX6 mutations. Am J Med Genet Part A 155(11):2821–2825. https://doi.org/10.1002/ajmg.a.34251
15. Suzuki K, Harada N, Yamane S et al (2013) Transcriptional regulatory factor X6 (Rfx6) increases gastric inhibitory polypeptide (GIP) expression in enteroendocrine K-cells and is involved in

GIP hypersecretion in high fat diet-induced obesity. J Biol Chem 288(3):1929–1938. https://doi.org/10.1074/jbc.M112.423137
16. Gehart H, van Es JH, Hamer K et al (2019) Identification of enteroendocrine regulators by real-time single-cell differentiation mapping. Cell 176(5):1158-1173, e1116. https://doi.org/10.1016/j.cell.2018.12.029
17. Ali G, Elsayed AK, Nandakumar M et al (2020) Keratinocytes derived from patient-specific induced pluripotent stem cells recapitulate the genetic signature of psoriasis disease. Stem Cells Dev 29(7):383–400. https://doi.org/10.1089/scd.2019.0150
18. Memon B, Elsayed AK, Bettahi I et al (2022) iPSCs derived from insulin resistant offspring of type 2 diabetic patients show increased oxidative stress and lactate secretion. Stem Cell Res Ther 13(1):428. https://doi.org/10.1186/s13287-022-03123-4
19. Elsayed AK, Younis I, Ali G, Hussain K, Abdelalim EM (2021) Aberrant development of pancreatic beta cells derived from human iPSCs with FOXA2 deficiency. Cell Death Dis 12(1):103. https://doi.org/10.1038/s41419-021-03390-8
20. Memon B, Younis I, Abubaker F, Abdelalim EM (2021) PDX1(-)/NKX6.1(+) progenitors derived from human pluripotent stem cells as a novel source of insulin-secreting cells. Diabetes Metab Res Rev 37(5):e3400. https://doi.org/10.1002/dmrr.3400
21. Memon B, Karam M, Al-Khawaga S, Abdelalim EM (2018) Enhanced differentiation of human pluripotent stem cells into pancreatic progenitors co-expressing PDX1 and NKX6.1. Stem Cell Res Ther 9(1):15. https://doi.org/10.1186/s13287-017-0759-z
22. Veres A, Faust AL, Bushnell HL et al (2019) Charting cellular identity during human in vitro beta-cell differentiation. Nature 569(7756):368–373. https://doi.org/10.1038/s41586-019-1168-5
23. Kong Y, Ebrahimpour P, Liu Y, Yang C, Alonso LC (2018) Pancreatic Islet Embedding for Paraffin Sections. J Vis Exp 136:57931. https://doi.org/10.3791/57931
24. Campbell-Thompson ML, Heiple T, Montgomery E, Zhang L, Schneider L (2012) Staining protocols for human pancreatic islets. J Vis Exp 63:e4068. https://doi.org/10.3791/4068
25. Zhu H, Wang G, Nguyen-Ngoc KV et al (2023) Understanding cell fate acquisition in stem-cell-derived pancreatic islets using single-cell multiome-inferred regulomes. Dev Cell 58(9):727–743 e711. https://doi.org/10.1016/j.devcel.2023.03.011
26. Aghadi M, Elgendy R, Abdelalim EM (2022) Loss of FOXA2 induces ER stress and hepatic steatosis and alters developmental gene expression in human iPSC-derived hepatocytes. Cell Death Dis 13(8):713. https://doi.org/10.1038/s41419-022-05158-0
27. Szklarczyk D, Franceschini A, Wyder S et al (2015) STRING v10: protein-protein interaction networks, integrated over the tree of life. Nucleic Acids Res 43(Database issue):D447–452. https://doi.org/10.1093/nar/gku1003
28. Trott J, Alpagu Y, Tan EK et al (2020) Mitchell-Riley syndrome iPSCs exhibit reduced pancreatic endoderm differentiation due to a mutation in RFX6. Development 147(21):dev194878. https://doi.org/10.1242/dev.194878
29. Krentz NAJ, Lee MYY, Xu EE et al (2018) Single-cell transcriptome profiling of mouse and hESC-derived pancreatic progenitors. Stem Cell Rep 11(6):1551–1564. https://doi.org/10.1016/j.stemcr.2018.11.008
30. Zito E, Chin KT, Blais J, Harding HP, Ron D (2010) ERO1-beta, a pancreas-specific disulfide oxidase, promotes insulin biogenesis and glucose homeostasis. J Cell Biol 188(6):821–832. https://doi.org/10.1083/jcb.200911086
31. Kahl R, Kampkötter A, Wätjen W, Chovolou Y (2004) Antioxidant enzymes and apoptosis. Drug Metab Rev 36(3–4):747–762. https://doi.org/10.1081/DMR-200033488
32. Zhu Z, Li QV, Lee K et al (2016) Genome editing of lineage determinants in human pluripotent stem cells reveals mechanisms of pancreatic development and diabetes. Cell Stem Cell 18(6):755–768. https://doi.org/10.1016/j.stem.2016.03.015
33. Ibrahim H, Balboa D, Saarimäki-Vire J et al (2024) *RFX6* haploinsufficiency predisposes to diabetes through impaired beta cell function. Diabetologia 2024. https://doi.org/10.1007/s00125-024-06163-y
34. Nakamura T, Fujikura J, Ito R, Keidai Y, Inagaki N (2024) Human *RFX6* regulates endoderm patterning at the primitive gut tube stage. PNAS Nexus 3(1):001. https://doi.org/10.1093/pnasnexus/page001
35. Sanchez JG, Rankin S, Paul E et al (2024) RFX6 regulates human intestinal patterning and function upstream of PDX1. Development 151(9):dev202529. https://doi.org/10.1242/dev.202529
36. Chen C, Fang R, Davis C, Maravelias C, Sibley E (2009) Pdx1 inactivation restricted to the intestinal epithelium in mice alters duodenal gene expression in enterocytes and enteroendocrine cells. Am J Physiol 297(6):G1126–1137. https://doi.org/10.1152/ajpgi.90586.2008
37. Yang YP, Magnuson MA, Stein R, Wright CV (2017) The mammal-specific Pdx1 Area II enhancer has multiple essential functions in early endocrine cell specification and postnatal beta-cell maturation. Development 144(2):248–257. https://doi.org/10.1242/dev.143123
38. Gao N, White P, Kaestner KH (2009) Establishment of intestinal identity and epithelial-mesenchymal signaling by Cdx2. Dev Cell 16(4):588–599. https://doi.org/10.1016/j.devcel.2009.02.010
39. Sharon N, Vanderhooft J, Straubhaar J et al (2019) Wnt signaling separates the progenitor and endocrine compartments during pancreas development. Cell Rep 27(8):2281–2291, e2285. https://doi.org/10.1016/j.celrep.2019.04.083
40. Weng C, Xi J, Li H et al (2020) Single-cell lineage analysis reveals extensive multimodal transcriptional control during directed beta-cell differentiation. Nat Metab 2(12):1443–1458. https://doi.org/10.1038/s42255-020-00314-2
41. Coykendall VMN, Qian MF, Tellez K et al (2023) RFX6 maintains gene expression and function of adult human islet α-cells. Diabetes 73(3):448–460. https://doi.org/10.2337/db23-0483
42. Tiedge M, Lortz S, Drinkgern J, Lenzen S (1997) Relation between antioxidant enzyme gene expression and antioxidative defense status of insulin-producing cells. Diabetes 46(11):1733–1742. https://doi.org/10.2337/diab.46.11.1733
43. Tiedge M, Lortz S, Munday R, Lenzen S (1998) Complementary action of antioxidant enzymes in the protection of bioengineered insulin-producing RINm5F cells against the toxicity of reactive oxygen species. Diabetes 47(10):1578–1585. https://doi.org/10.2337/diabetes.47.10.1578
44. Jorns A, Tiedge M, Lenzen S, Munday R (1999) Effect of superoxide dismutase, catalase, chelating agents, and free radical scavengers on the toxicity of alloxan to isolated pancreatic islets in vitro. Free Radic Biol Med 26(9–10):1300–1304. https://doi.org/10.1016/s0891-5849(98)00325-6
45. Goth L (2008) Catalase deficiency and type 2 diabetes. Diabetes Care 31(12):e93. https://doi.org/10.2337/dc08-1607